Supplementary Information

$KLi_2RE(BO_3)_2$ (RE = Dy, Ho, Er, Tm, Yb and Y): structural, spectroscopic and thermogravimetric studies on a series of mixed alkali rare-earth orthoborates

Pengyun Chen[1], M. Mangir Murshed[1,4*], Michael Fischer[2,4], Thomas Frederichs[3], Thorsten M. Gesing[1,4]

[1]University of Bremen, Institute of Inorganic Chemistry and Crystallography, Faculty of Biology and Chemistry, Leobener Straße 7, D-28359 Bremen, Germany

[2]University of Bremen, Crystallography, Faculty of Geosciences, Klagenfurter Straße 2-4, D-28359 Bremen, Germany

[3]University of Bremen, Faculty of Geosciences, Klagenfurter Straße 2-4, D-28359 Bremen, Germany

[4]University of Bremen, MAPEX Center for Materials and Processes, Bibliothekstraße 1, D-28359 Bremen, Germany

*Corresponding author: e-mail address: murshed@uni-bremen.de, phone: +49 (0)421 218 63144, fax: +49 421 218 63145.

Table S1: Atomic coordinates, equivalent isotropic displacement parameters (U_{eq} /10^4pm^2), and bond valence sum (BVS /v.u.) of $KLi_2RE(BO_3)_2$. U_{eq} is defined as one-third of the trace of the U_{ij} tensor components. All atoms are in the *4e* Wyckoff.

Atom	*x*	*y*	*z*	U_{eq}	BVS
			$KLi_2Dy(BO_3)_2$		
Dy	0.53708(2)	0.88265(2)	0.34218(2)	0.00483(2)	2.81(1)
K	0.57478(7)	0.37572(5)	0.41357(4)	0.01071(7)	1.46(1)
B1	0.6471(3)	0.8590(2)	0.7634(2)	0.0068(3)	2.86(1)
B2	0.6301(3)	0.6296(2)	0.2148(2)	0.0061(3)	2.93(1)
Li1	0.4182(6)	0.8835(4)	0.9944(4)	0.0120(6)	1.13(1)
Li2	0.4174(6)	0.3842(4)	0.0495(4)	0.0132(7)	0.95(1)
O1	0.7220(2)	0.72711(14)	0.81783(15)	0.0075(2)	-2.00(1)
O2	0.6002(2)	0.96401(14)	0.85915(15)	0.0081(2)	-2.01(1)
O3	0.6014(2)	0.89412(15)	0.60856(15)	0.0095(2)	-1.88(1)
O4	0.6565(2)	0.49831(14)	0.14945(15)	0.0074(2)	-2.00(1)
O5	0.5732(2)	0.74754(14)	0.12375(15)	0.0089(2)	-2.10(1)
O6	0.6594(2)	0.65034(15)	0.36933(15)	0.0091(2)	-2.15(1)
			$KLi_2Er(BO_3)_2$		
Er	0.53739(2)	0.88315(2)	0.34192(2)	0.00536(4)	2.87(1)
K	0.57422(7)	0.37571(4)	0.41403(5)	0.01082(8)	1.50(1)
B1	0.6491(3)	0.8593(2)	0.7621(2)	0.0069(3)	2.86(1)
B2	0.6320(3)	0.6298(2)	0.2153(2)	0.0068(3)	2.93(1)
Li1	0.4171(7)	0.8826(4)	0.9945(5)	0.0132(7)	1.15(1)
Li2	0.4167(7)	0.3853(4)	0.0502(5)	0.0132(7)	0.94(1)
O1	0.7253(2)	0.72683(15)	0.81675(17)	0.0080(2)	-2.02(1)
O2	0.6001(2)	0.96430(16)	0.85810(16)	0.0089(2)	-2.02(1)
O3	0.6028(3)	0.89482(16)	0.60672(17)	0.0103(3)	-1.89(1)
O4	0.6584(2)	0.49800(15)	0.14996(17)	0.0077(2)	-2.03(1)
O5	0.5746(2)	0.74868(16)	0.12402(17)	0.0092(2)	-2.11(1)
O6	0.6600(2)	0.65146(16)	0.37052(17)	0.0093(2)	-2.18(1)
			$KLi_2Tm(BO_3)_2$		
Tm	0.53721(2)	0.88334(2)	0.34175(2)	0.00472(4)	3.06(1)

K	0.57512(10)	0.37571(7)	0.41441(7)	0.01183(12)	1.54(1)
B1	0.6485(5)	0.8591(3)	0.7612(4)	0.0062(5)	2.86(2)
B2	0.6323(5)	0.6300(3)	0.2155(4)	0.0071(5)	2.95(2)
Li1	0.4179(8)	0.8835(6)	0.9950(6)	0.0136(10)	1.16(1)
Li2	0.4146(8)	0.3857(6)	0.0501(6)	0.0136(10)	0.95(1)
O1	0.7257(3)	0.7260(2)	0.8159(2)	0.0074(4)	-2.05(1)
O2	0.5992(3)	0.9639(2)	0.8575(2)	0.0076(4)	-2.07(1)
O3	0.6016(3)	0.8952(2)	0.6054(2)	0.0097(4)	-1.95(1)
O4	0.6592(3)	0.4975(2)	0.1501(2)	0.0071(4)	-2.07(1)
O5	0.5756(3)	0.7489(2)	0.1242(2)	0.0091(4)	-2.16(1)
O6	0.6589(3)	0.6517(2)	0.3706(2)	0.0094(4)	-2.22(1)
$KLi_2Yb(BO_3)_2$					
Yb	0.53733(2)	0.88369(2)	0.34144(2)	0.00474(3)	2.85(1)
K	0.57460(8)	0.37563(5)	0.41460(5)	0.01035(8)	1.54(1)
B1	0.6501(3)	0.8593(2)	0.7609(2)	0.0058(3)	2.87(1)
B2	0.6323(3)	0.6305(2)	0.2155(3)	0.0062(3)	2.94(2)
Li1	0.4191(8)	0.8830(5)	0.9952(5)	0.0154(8)	1.17(1)
Li2	0.4152(7)	0.3859(5)	0.0508(5)	0.0134(8)	0.94(1)
O1	0.7268(2)	0.72642(16)	0.81537(17)	0.0074(2)	-2.03(1)
O2	0.5993(2)	0.96458(17)	0.85708(17)	0.0083(3)	-2.04(1)
O3	0.6031(3)	0.89628(17)	0.60504(18)	0.0096(3)	-1.88(1)
O4	0.6599(2)	0.49777(16)	0.15072(18)	0.0072(2)	-2.04(1)
O5	0.5754(2)	0.74960(17)	0.12390(17)	0.0089(3)	-2.14(1)
O6	0.6598(2)	0.65330(17)	0.37112(17)	0.0087(3)	-2.18(1)
$KLi_2Y(BO_3)_2$					
Y	0.53708(4)	0.88293(3)	0.34189(3)	0.00516(7)	3.04(1)
K	0.57467(9)	0.37586(7)	0.41398(6)	0.01089(12)	1.47(1)
B1	0.6480(4)	0.8591(3)	0.7628(3)	0.0066(5)	2.85(2)
B2	0.6319(4)	0.6296(3)	0.2146(3)	0.0072(5)	2.93(2)
Li1	0.4171(7)	0.8831(6)	0.9934(5)	0.0125(9)	1.13(1)
Li2	0.4172(8)	0.3851(6)	0.0502(5)	0.0142(10)	0.93(1)
O1	0.7239(3)	0.72693(19)	0.8169(2)	0.0073(4)	-2.04(1)
O2	0.6000(3)	0.9640(2)	0.8587(2)	0.0084(4)	-2.04(1)

O3	0.6014(3)	0.8945(2)	0.6074(2)	0.0098(4)	-1.93(1)
O4	0.6584(3)	0.4983(2)	0.1495(2)	0.0074(4)	-2.05(1)
O5	0.5739(3)	0.7481(2)	0.1238(2)	0.0092(4)	-2.11(1)
O6	0.6597(3)	0.65126(19)	0.3696(2)	0.0088(4)	-2.19(1)

Table S2. Energy dispersive X-ray (EDX) analysis results on three different single crystals of each $KLi_2RE(BO_3)_2$ (RE = Dy, Ho, Er, Tm, Yb and Y) compound, showing the K:RE atomic ratio.

Compound	**K : RE**		
	Crystal-1	**Crystal-2**	**Crystal-3**
$KLi_2Dy(BO_3)_2$	1.03(3) : 1.00(10)	1.00(3) :1.00(10)	1.04(2) : 1.00(6)
$KLi_2Ho(BO_3)_2$	1.11(3) : 1.00(9)	1.06(3) : 1.00(9)	1.03(3) : 1.00(9)
$KLi_2Er(BO_3)_2$	1.05(4) :1.00(13)	1.03(2) : 1.00(8)	1.00(3) : 1.00(10)
$KLi_2Tm(BO_3)_2$	1.01(2) : 1.00(9)	1.06(2) : 1.00(7)	1.08(2) : 1.00(7)
$KLi_2Yb(BO_3)_2$	1.01(2) : 1.00(8)	1.17(3) : 1.00(9)	1.13(2) : 1.00(7)
$KLi_2Y(BO_3)_2$	1.12(3) : 1.00(8)	0.91(2) :1.00(7)	1.05(3) : 1.00(8)

Table S3: Structural comparison between "312"-type rare-earth borates in terms of space group (*SG*), sum of ionic radii of alkali-metals (Σ in units of pm), metric parameter (*a, b* and *c* in units of pm and *β* in degree), coordination and their connectivity.

Formula	***SG***	**Σ**	**Metric**	**Coordination**	**Structural details**	**Reference**
$Li_3Sc(BO_3)_2$	$P2_1/n$	177	*a* = 478.3(2) *b* = 595.4(2) *c* = 816.3(3) *β* = 90.70(1)	ScO_6 octahedra BO_3 triangle LiO_4 tetrahedra LiO_4 rectangle	Isolated ScO_6 octahedra are linked via LiO_4 rectangles along ***b*** axis, further bridged by LiO_4 tetrahedra and BO_3 triangles	(1)
$Li_3Gd(BO_3)_2$	$P2_1/n$	177	*a* = 992.3 *b* = 642.5 *c* = 872.4 *β* = 114.815	GdO_8 dodecahedra BO_3 triangle LiO_4 tetrahedra	Layers of $[Gd_2O_{14}]$ clusters connected by BO_3 triangles with LiO_4 tetrahedra inserted into the cavity.	(2)
$KLi_2Ho(BO_3)_2$	$P2_1/n$	269	*a* = 671.112(5) *b* = 931.737(6) *c* = 899.091(6) *β* = 102.8257(6)	HoO_7 pentagonal bipyramid BO_3 triangle KO_8 dodecahedra LiO_4 tetrahedra	$[Ho_2(BO_3)_4O_4]^{14-}$ anionic clusters connected to each other by corner sharing, with KO_8 dodecahedra and LiO_4 tetrahedra filled into the voids	This work
$Na_3Gd(BO_3)_2$	$P2_1/n$	313	*a* = 1014.8 *b* = 872.83 *c* = 652.3 *β* = 89.12	GdO_8 dodecahedra BO_3 triangles NaO_7 monocapped octahedra NaO_6 triangle prism, NaO_4 tetrahedra	Edge-shared $[GdO_5B(1)O_3]$ chains form 2-dimensional layer, which are further bridged by the $B(2)O_3$ triangles and NaO_x polyhedra.	(3)
$Rb_2LiNd(BO_3)_2$	*Pbcm*	363	*a* = 711.3(2) *b* = 969.1(3) *c* = 1013.5(3)	NdO_8 dodecahedra BO_3 triangle RbO_5 pentagonal pyramid LiO_4 tetrahedra	Corner-shared $[NdO_5B(1)O_3]$ chains are reinforced by $B(2)O_3$ groups to build up $[Nd_4B_4O_{24}]_n$ layers in the *bc* plane.	(4)
$K_3Sm(BO_3)_2$	*Pnma*	414	*a* = 904.6(3) *b* = 710.0(2) *c* = 1118.6(3)	SmO_7 pentagonal bipyramid KO_6 octahedra KO_6 triangle prism	$B(1)O_3$ triangle bridges three $[SmO_4B(2)O_3]$ chains in a scaffolding-like way with KO_6 residing the interstitials	(5)
$K_3Y(BO_3)_2$	*Pnnm*	414	*a* = 933.77(9) *b* = 677.01(6) *c* = 550.58(4)	YO_6 octahedra BO_3 triangle KO_6 octahedra KO_6 hexagons	Isolated YO_6 octahedra use all oxygen atoms sharing with BO_3 groups to form a 3-dimensional framework.	(5)
$Cs_2LiNd(BO_3)_2$	*Pbcm*	446	*a* =721.13(3) *b* = 996.21(4) *c* = 1033.47(4)	NdO_8 dodecahedra BO_3 triangle CsO_5 pentagonal pyramid LiO_4 tetrahedra	Isostructural to $Rb_2LiNd(BO_3)_2$	(4)

Table S4: Phases identified from the X-ray powder data Rietveld refinement during the synthesis trials of $ALi_2RE(BO_3)_2$ (A = Rb and Cs, RE = Eu, Gd, Tb, Lu, Sc and In) compounds.

Target compound	Observed phase/phases
$KLi_2Eu(BO_3)_2$	$Li_6Eu(BO_3)_3$
$KLi_2Gd(BO_3)_2$	$Li_6Gd(BO_3)_3$
$KLi_2Tb(BO_3)_2$	$Li_6Tb(BO_3)_3$
$KLi_2Lu(BO_3)_2$	$K_3Lu(BO_3)_2$ and $LuBO_3$
$KLi_2Sc(BO_3)_2$	$Li_3Sc(BO_3)_2$, $LiScO_2$ and KBO_2
$KLi_2In(BO_3)_2$	In_2O_3
$RbLi_2Er(BO_3)_2$	$Li_6Er(BO_3)_3$ and $ErBO_3$
$RbLi_2Yb(BO_3)_2$	$Li_6Yb(BO_3)_2$ and $YbBO_3$
$CsLi_2Er(BO_3)_2$	$Li_6Er(BO_3)_3$ and $ErBO_3$
$CsLi_2Yb(BO_3)_2$	$Li_6Yb(BO_3)_2$ and $YbBO_3$

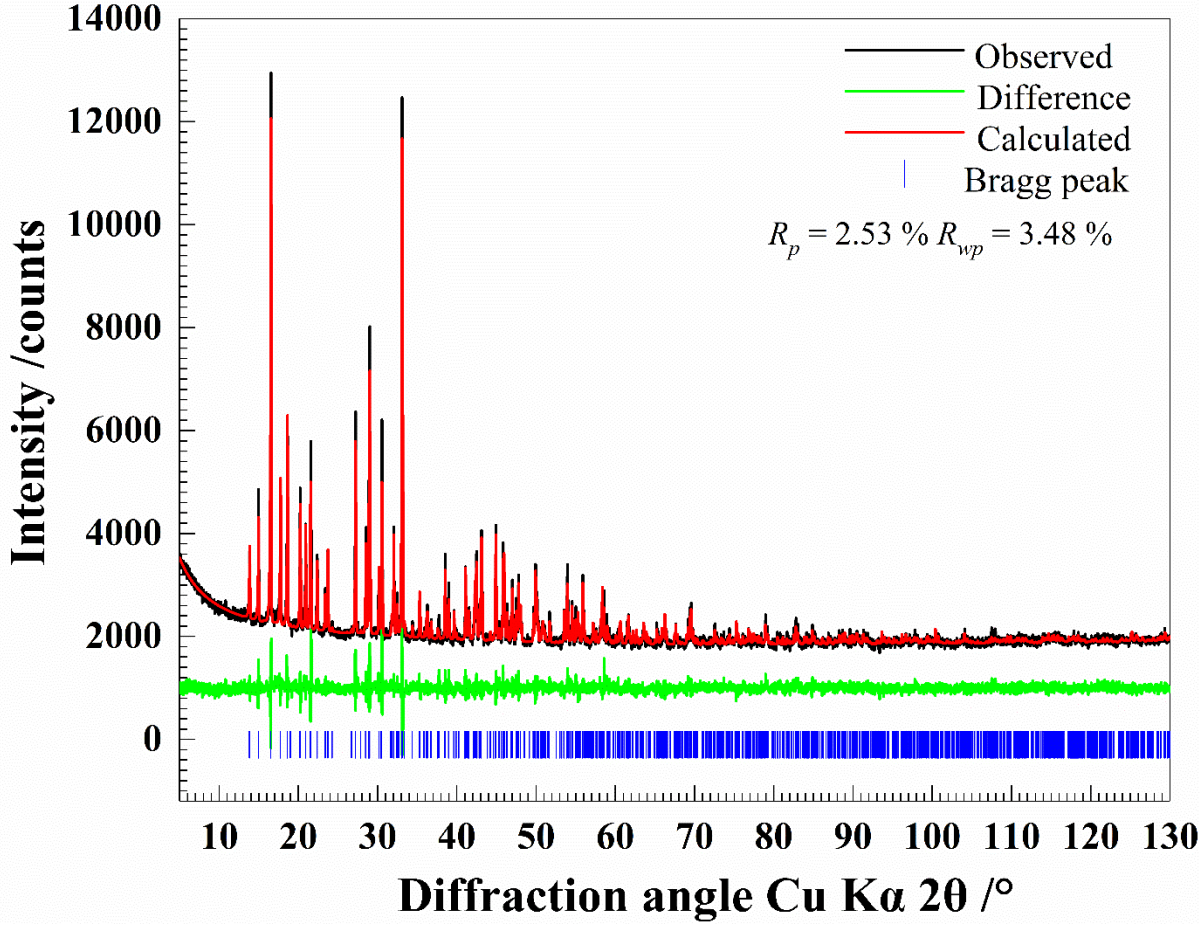

Figure S1: X-ray powder data Rietveld plot of $KLi_2Dy(BO_3)_2$.

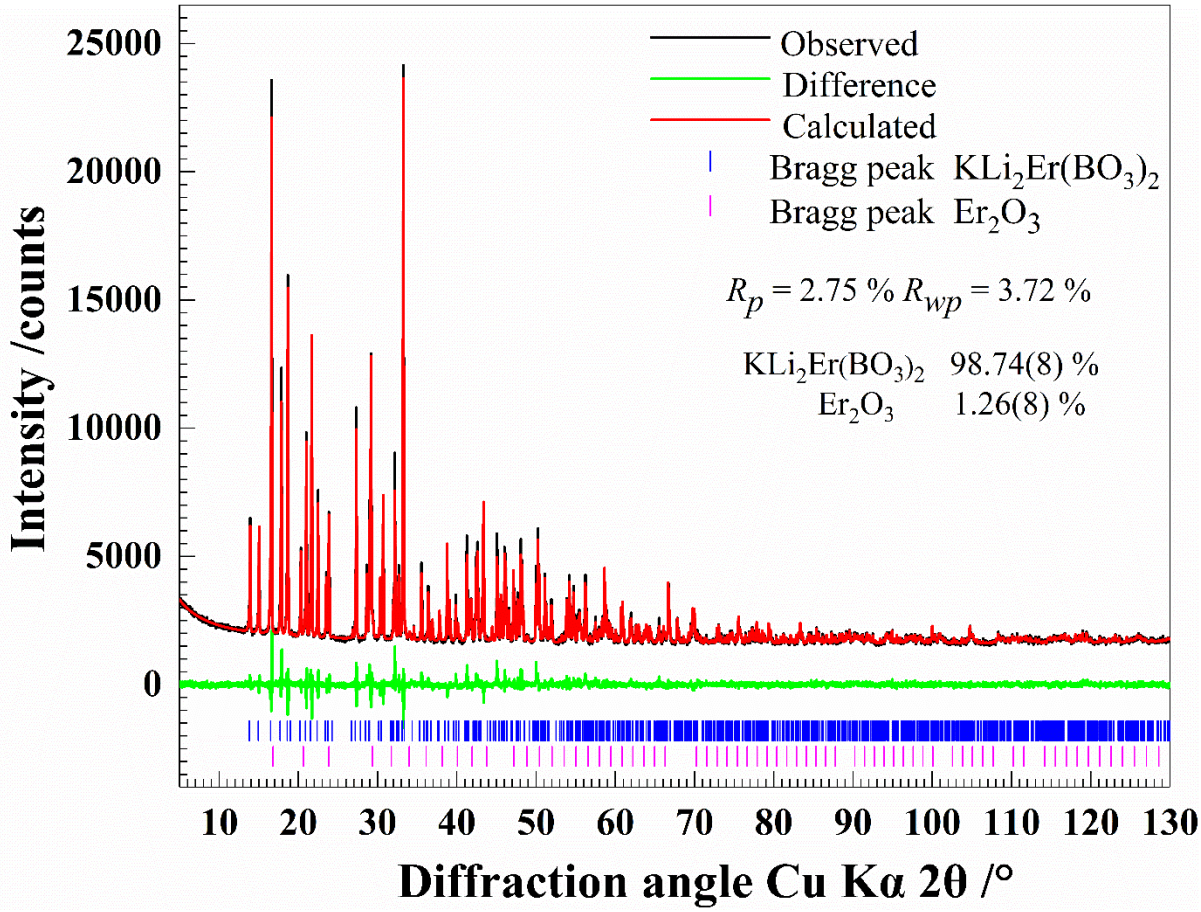

Figure S2: X-ray powder data Rietveld plot of $KLi_2Er(BO_3)_2$.

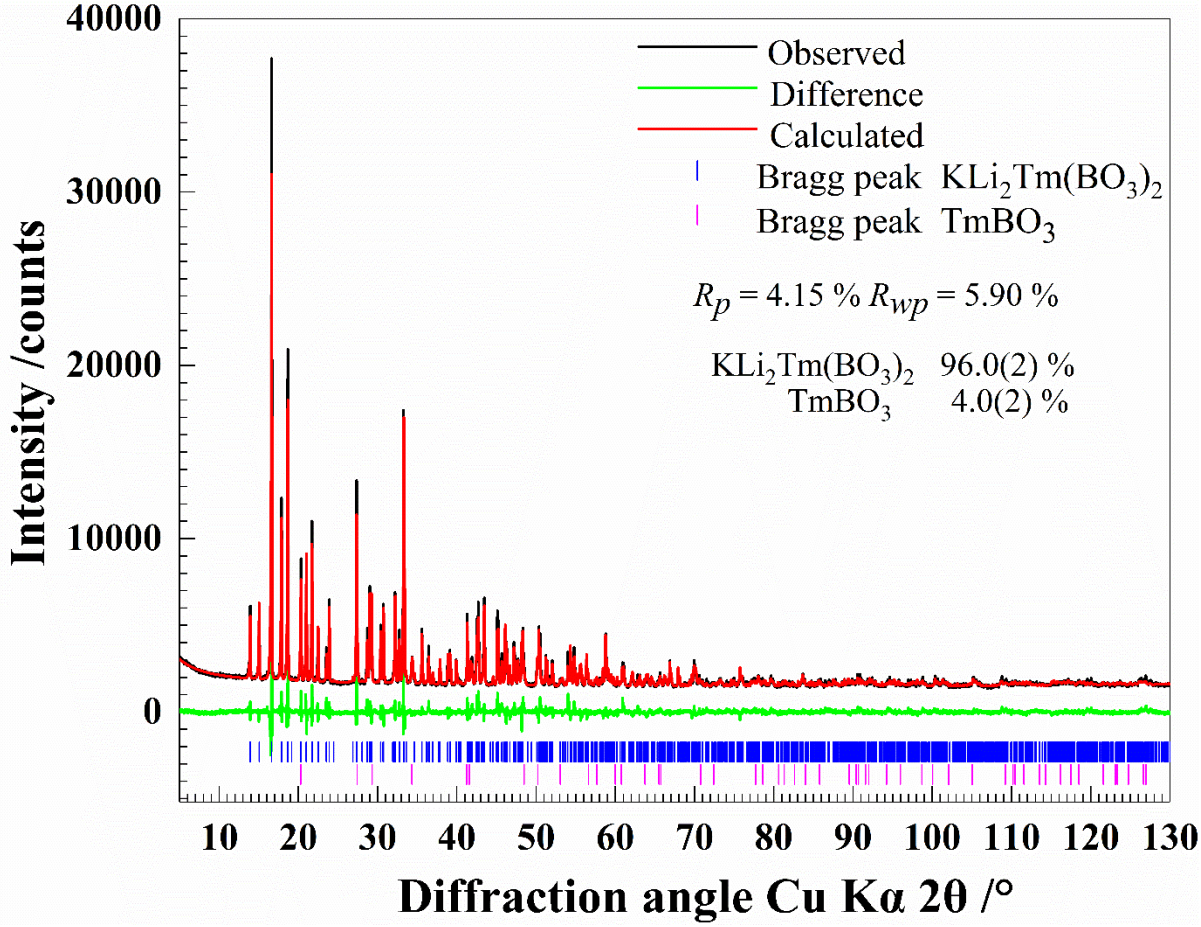

Figure S3: X-ray powder data Rietveld plots of $KLi_2Tm(BO_3)_2$

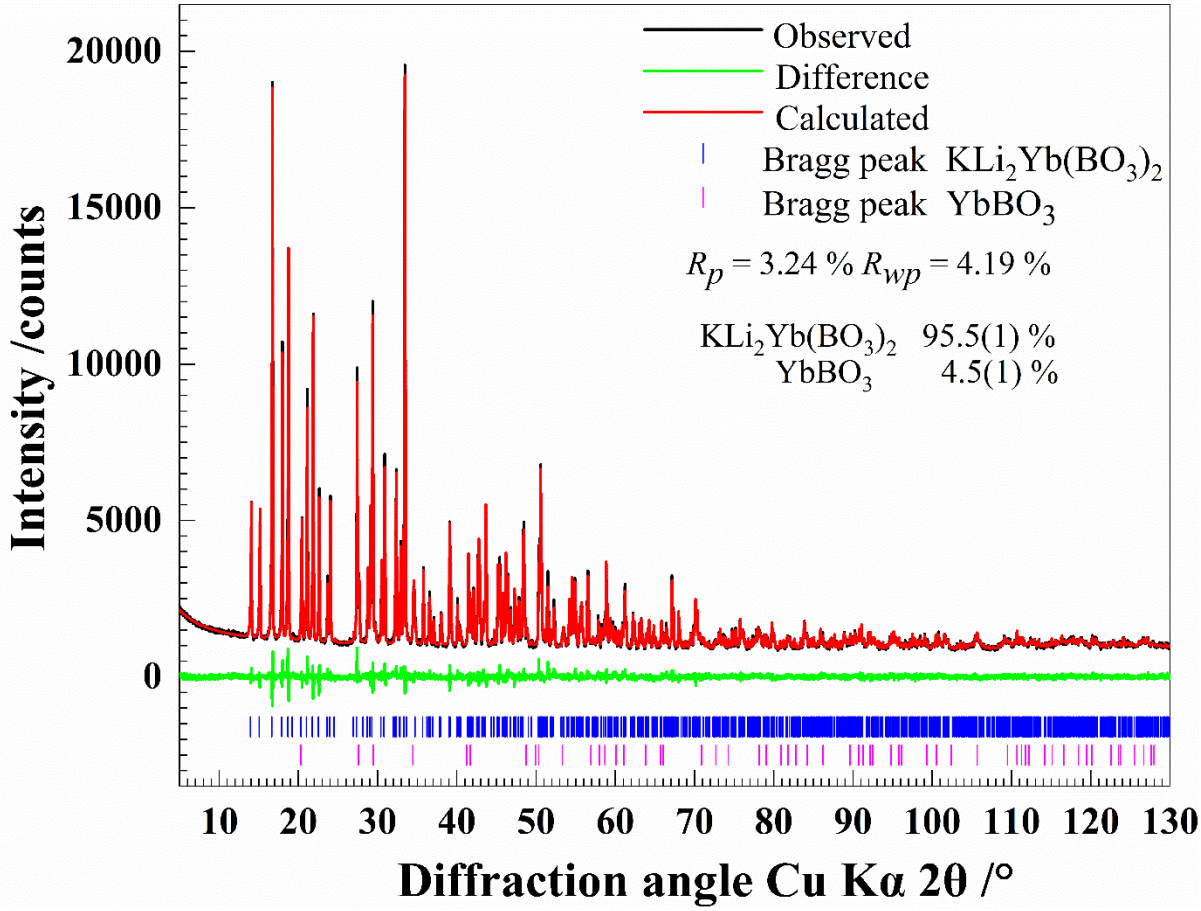

Figure S4: X-ray powder data Rietveld plot of $KLi_2Yb(BO_3)_2$.

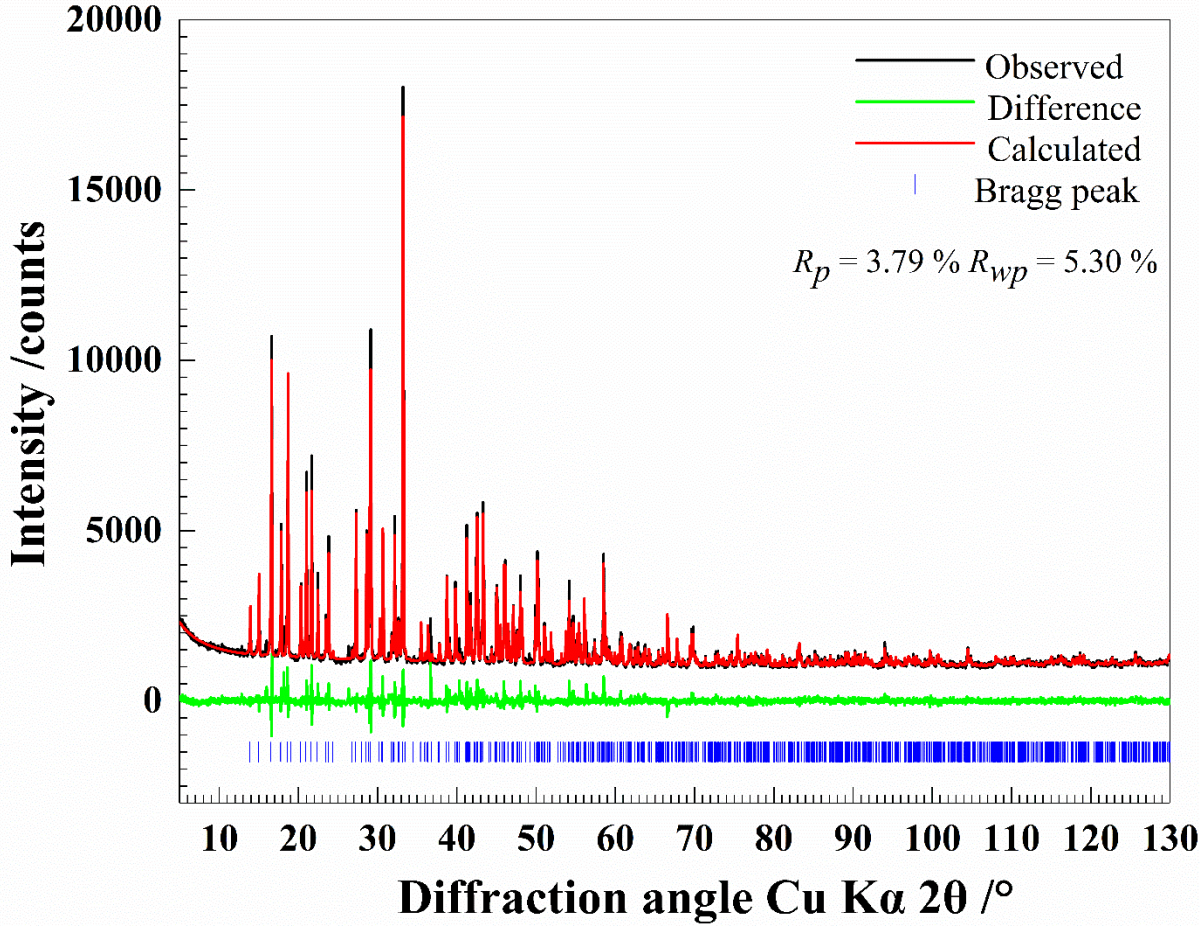

Figure S5: X-ray powder data Rietveld plots of $KLi_2Y(BO_3)_2$.

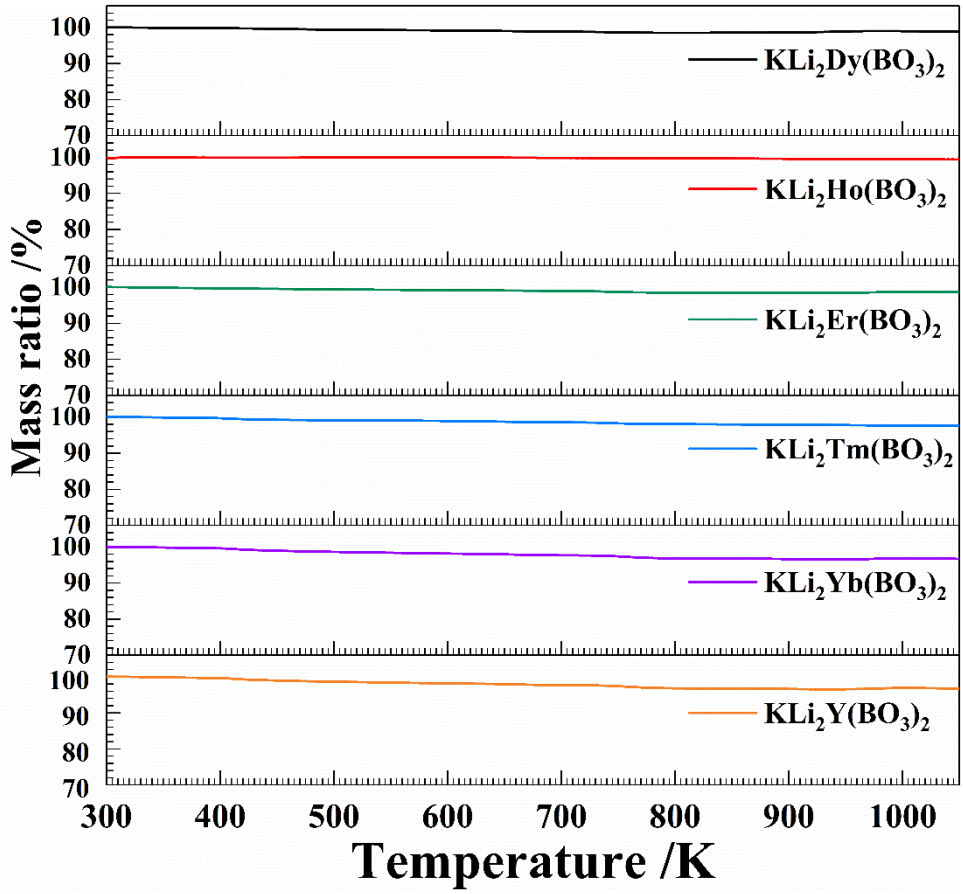

Figure S6: Thermal gravimetric analysis (TGA) curves of $KLi_2RE(BO_3)_2$.

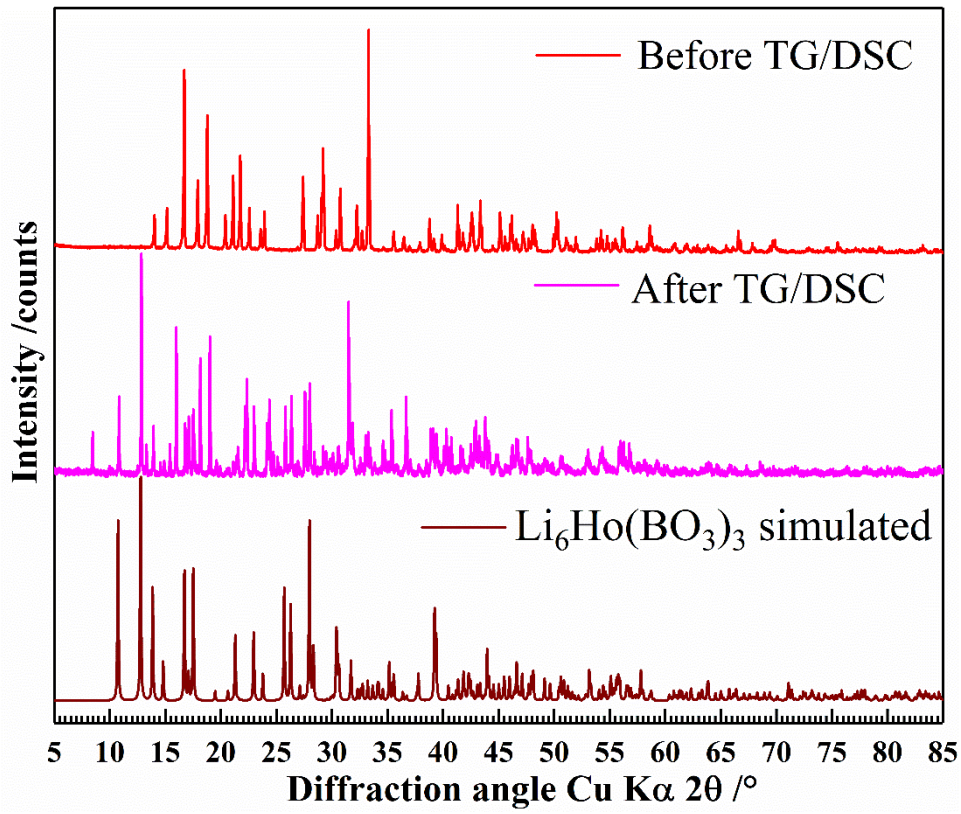

Figure S7: Powder XRD patterns of $KLi_2Ho(BO_3)_2$ before and after the TG/DSC. The simulated XRD pattern of $Li_6Ho(BO_3)_3$ is only for comparison.

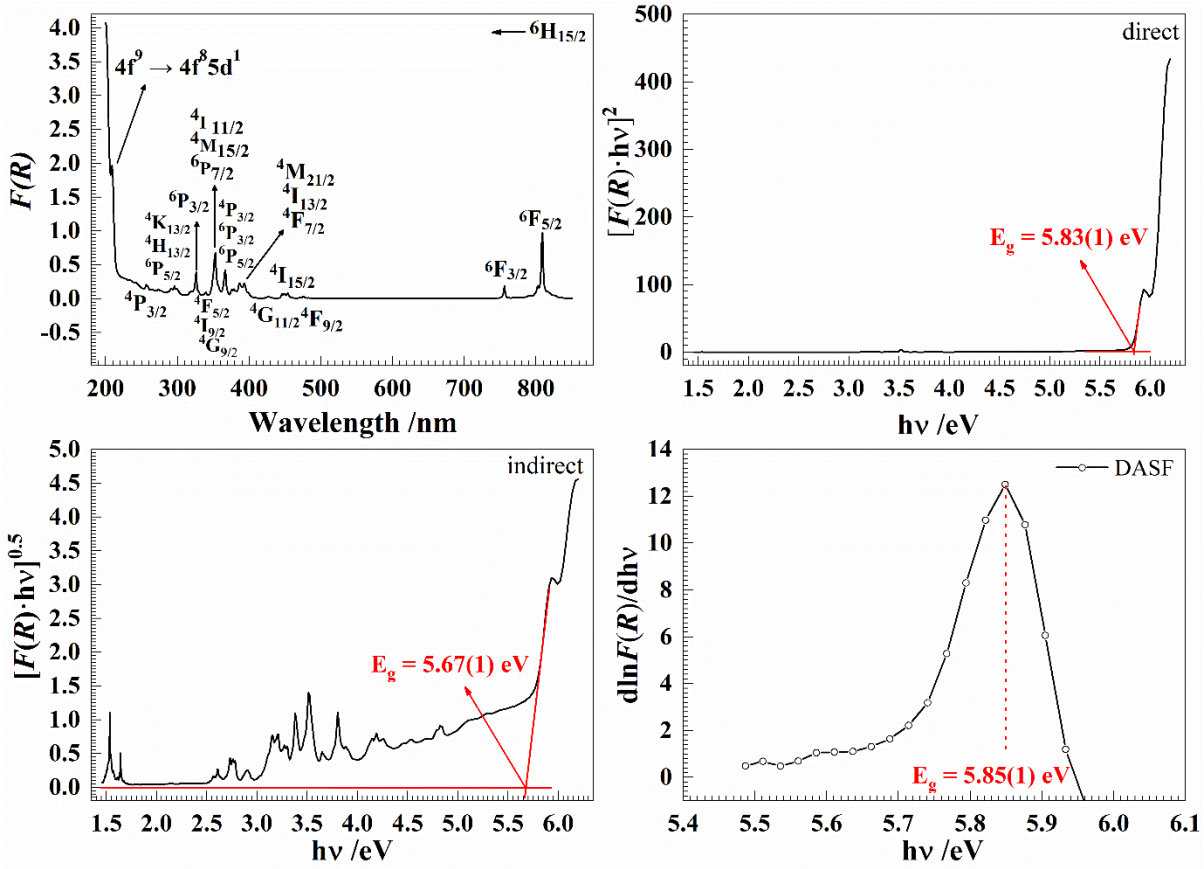

Figure S8: Kubelka-Munk transformed diffuse reflectance spectrum (DRS) of $KLi_2Dy(BO_3)$ (top left), Tauc plots for indirect (bottom left) and direct (top right) optical transitions, and DASF plot (bottom right).

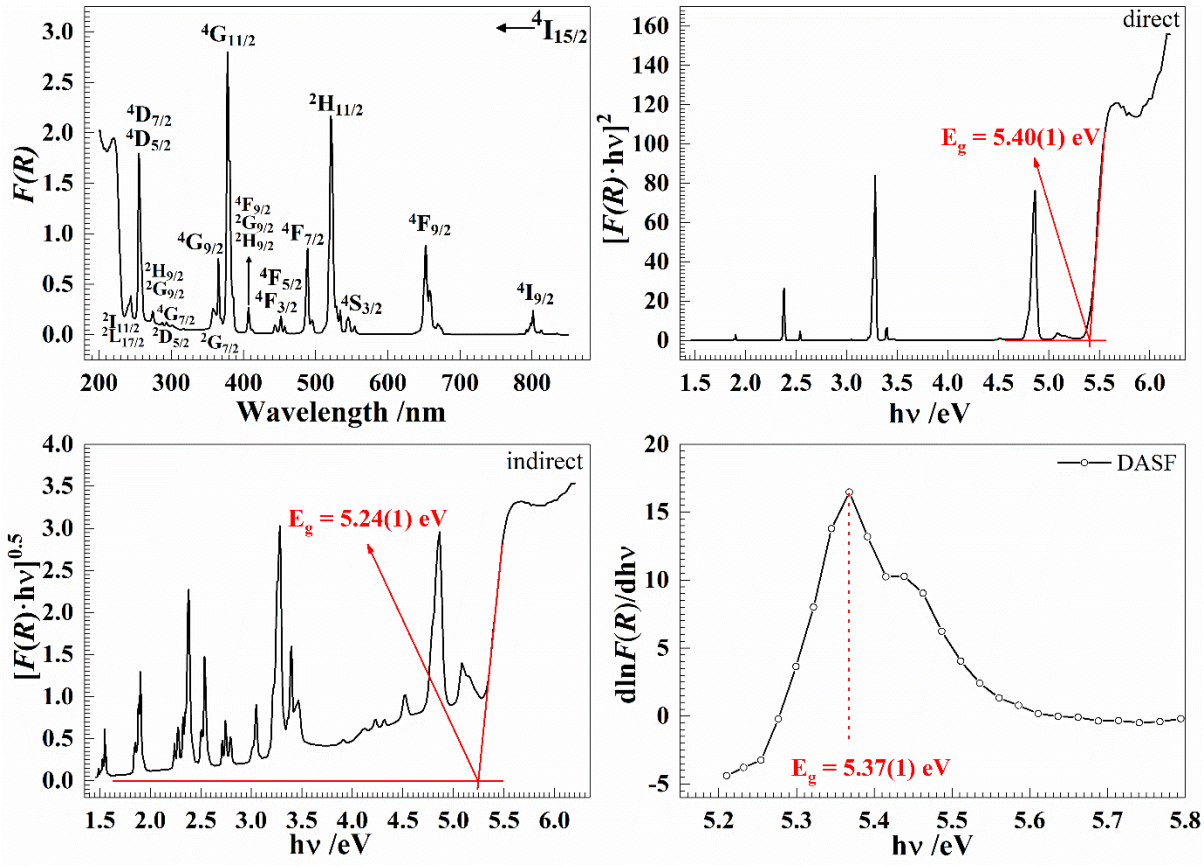

Figure S9: Kubelka-Munk transformed diffuse reflectance spectrum of $KLi_2Er(BO_3)$ (top left), Tauc plots for indirect (bottom left) and direct (top right) optical transitions, and DASF plot (bottom right).

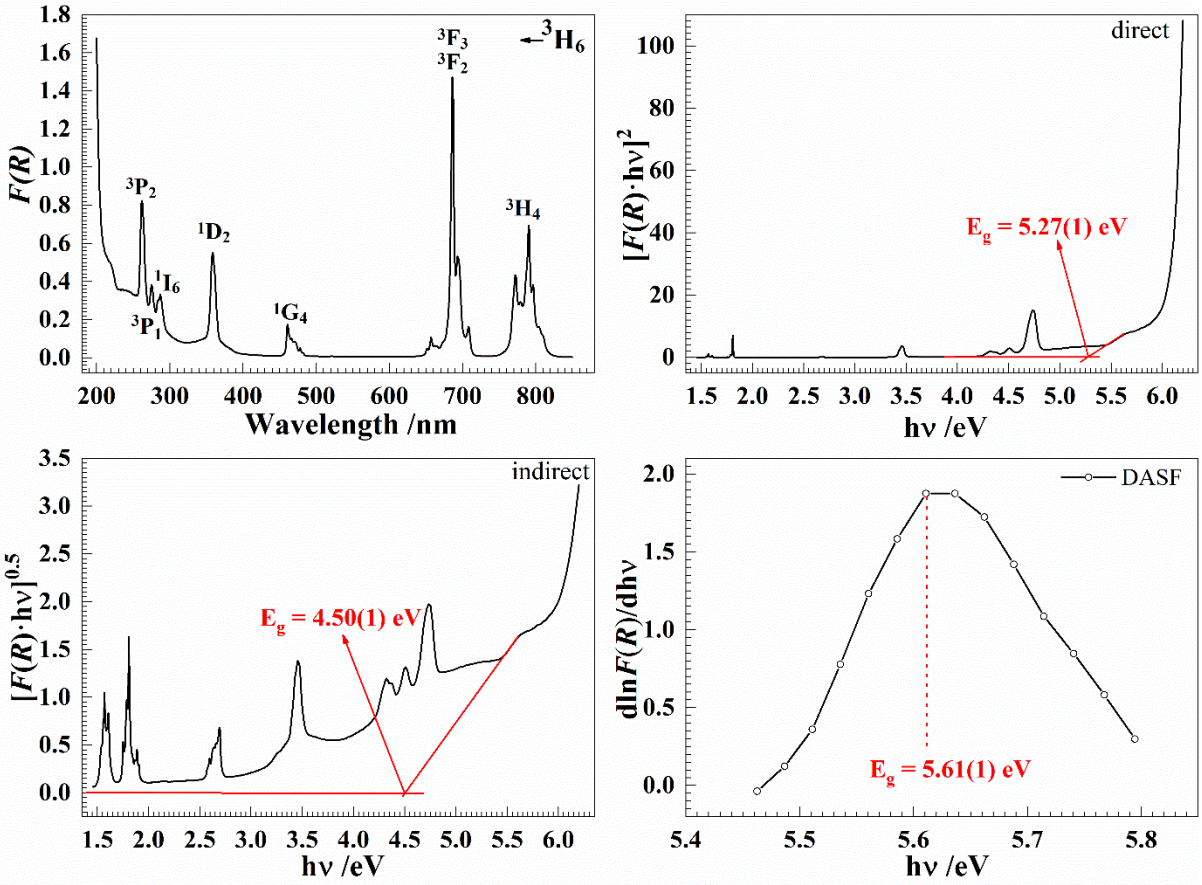

Figure S10: Kubelka-Munk transformed diffuse reflectance spectrum of $KLi_2Tm(BO_3)$ (top left), Tauc plots for indirect (bottom left) and direct (top right) optical transitions, and DASF plot (bottom right).

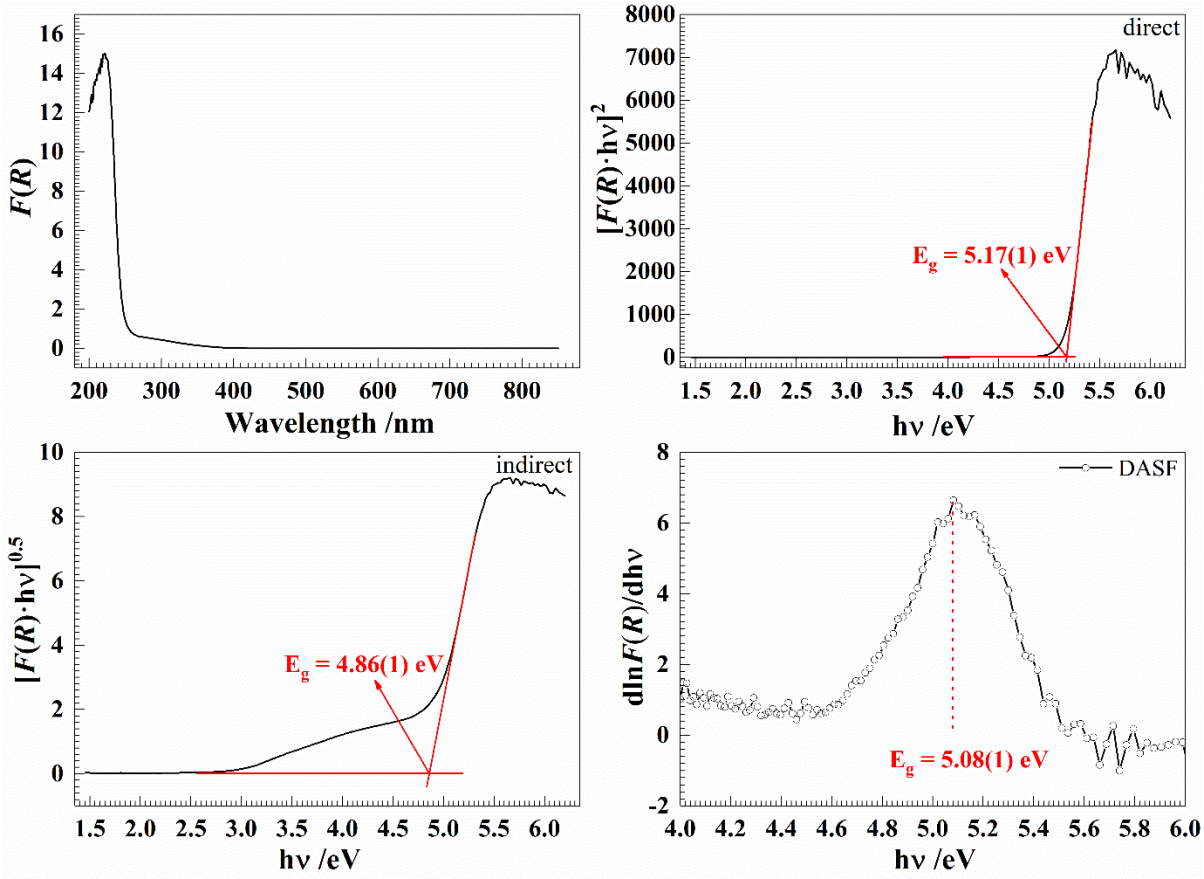

Figure S11: Kubelka-Munk transformed diffuse reflectance spectrum of $KLi_2Yb(BO_3)$ (top left), Tauc plots for indirect (bottom left) and direct (top right) optical transitions, and DASF plot (bottom right).

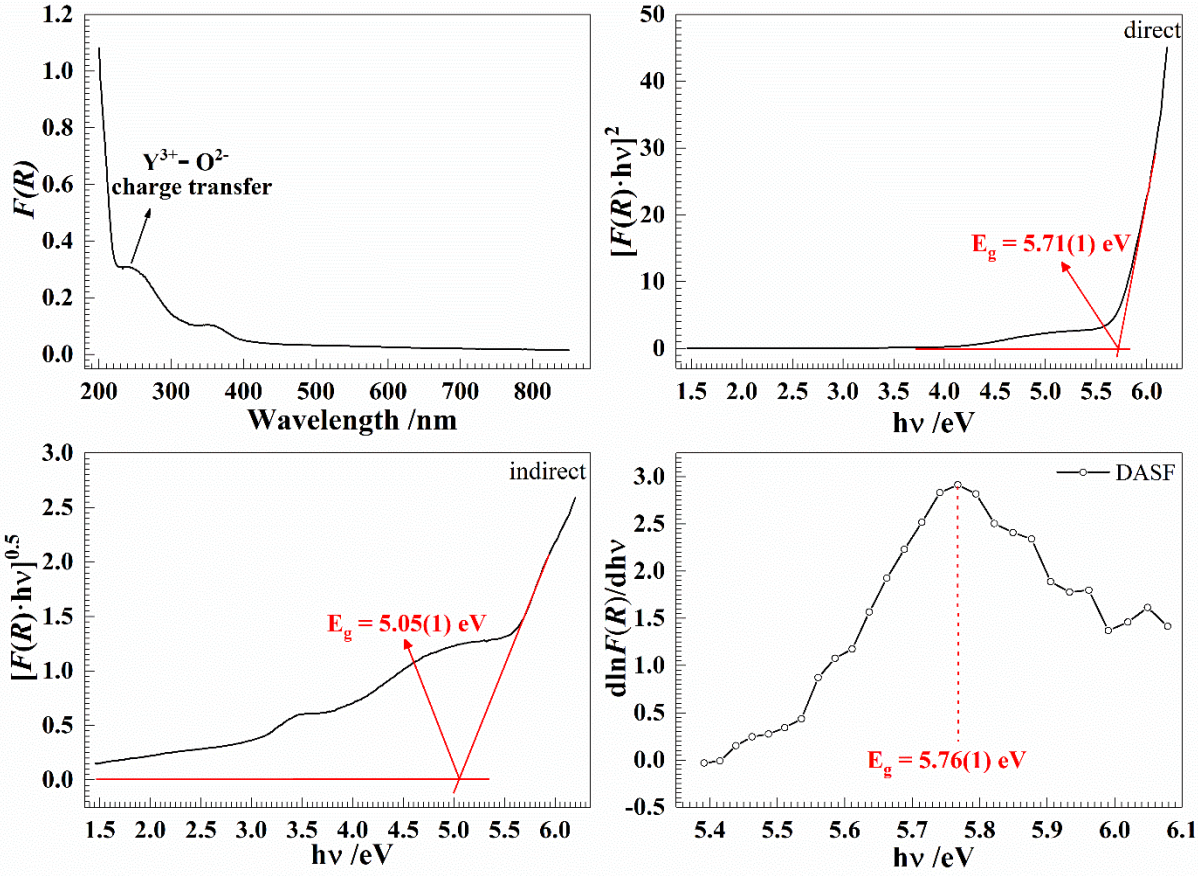

Figure S12: Kubelka-Munk transformed diffuse reflectance spectrum of $KLi_2Y(BO_3)$ (top left), Tauc plots for indirect (bottom left) and direct (top right) optical transitions, and DASF plot (bottom right).

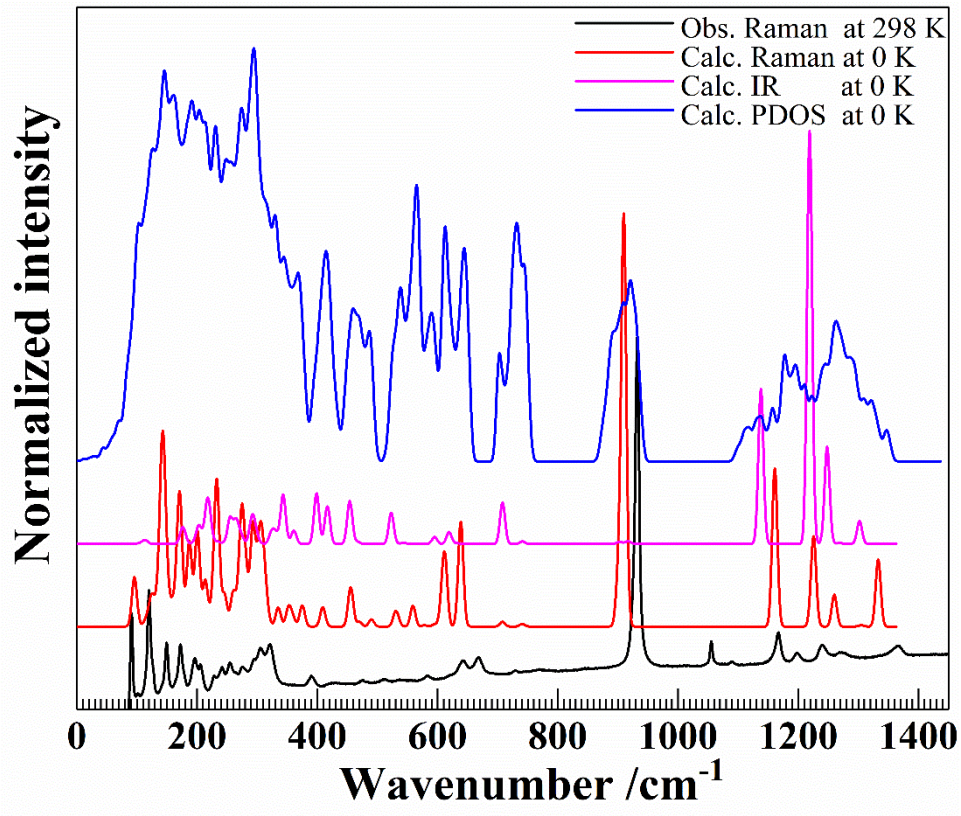

Figure S13: Comparative view between the phonon density of states (PDOS), Raman and infrared (IR) spectra of $KLi_2Y(BO_3)_2$.

References

(1) Mao, L.; Zhou, T.; Ye, N., Trilithium scandium bis (orthoborate), *Acta Crystallogr., Sect. E,* **2008,** *64*, i38-i38.

(2) Jubera, V.; Gravereau, P.; Chaminade, J. P., Crystal structure of the new borate $Li_3Gd(BO_3)_2$: Comparison with the homologous $Na_3Ln(BO_3)_2$ (Ln: La, Nd) compounds, *Solid State Sci.*, **2001,** *3*, 469-475.

(3) Naidu, S. A.; Boudin, S.; Varadaraju, U.; Raveau, B., Influence of structural distortions upon photoluminescence properties of Eu^{3+} and Tb^{3+} activated $Na_3Ln(BO_3)_2$ (Ln = Y, Gd) borates, *J. Solid State Chem.,* **2012,** *190*, 186-190.

(4) Chen, P.; Xia, M.; Li, R., Mixed Alkali Neodymium Orthoborates: $K_9Li_3Nd_3(BO_3)_7$ and $A_2LiNd(BO_3)_2$ (A = Rb, Cs), *Z. Anorg. Allg. Chem.*, **2016,** *642*, 424-430.

(5) Gao, J.; Li, R., Potassium rich rare earth (RE) borates $K_3RE(BO_3)_2$, *Solid State Sci.,* **2008,** *10*, 26-30.